Taylor & Francis
Taylor & Francis Group

REVIEW ARTICLE

OPEN ACCESS · Check for updates

Imaging technologies and strategies for detection of extant extraterrestrial microorganisms

Jay L. Nadeau[a,b], Manuel Bedrossian[a] and Christian A. Lindensmith[c]

[a]Graduate Aerospace Laboratories, California Institute of Technology, Pasadena, CA, USA; [b]Department of Physics, Portland State University, Portland, OR, USA; [c]Jet Propulsion Laboratory, California Institute of Technology, Pasadena, CA, USA

ABSTRACT

There is no reductionist definition of life, so the way organisms look, behave, and move is the most definitive way to identify extraterrestrial life. Life elsewhere in the Solar System is likely to be microbial, but no microscope capable of imaging prokaryotic life has ever flown on a lander mission to a habitable planet. Nonetheless, high-resolution microscopes have been developed that are appropriate for planetary exploration. Traditional light microscopy, interferometric microscopy, light-field microscopy, scanning probe microscopy, and electron microscopy are all possible techniques for the detection of extant micro-organisms on Mars and the moons of Jupiter and Saturn. This article begins with a general discussion of the challenges involved in searching for prokaryotic life, then reviews instruments that have flown, that have been selected for flight but not flown or not flown yet, and developing techniques of great promise for life detection that have not yet been selected for flight.
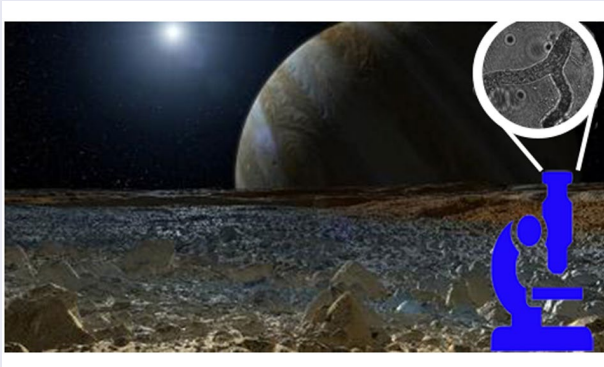
CONTACT Jay L. Nadeau ✉ nadeau@pdx.edu

Introduction

Scope of the problem

There is no current instrumentation qualified for space flight that can definitively detect extant prokaryotic life from a cubic meter of Earth ocean water.

The reasons are multiple. No NASA mission since Viking in 1978 has attempted to find extant extraterrestrial life [1]. Five lander missions to Mars have successfully deployed since Viking, but until 2015 [2] it was believed that Mars had no liquid water at present at or near its surface, so missions have been explicitly designed to seek signs of present or past 'habitability' – not life. Habitability mostly refers to mineral characterization to infer the past or present existence of liquid water.

Over the past few years, interest has expanded from the Mars surface to also include the subsurface [3–7], where water is suspected to exist, and the so-called Ocean Worlds – Europa, Enceladus, and Ganymede [8]. These moons of Jupiter and Saturn have extensive subsurface water oceans. NASA now has a congressional mandate to search for extant life on Europa, where a global ocean exists below a shell of ice several kilometers thick. Attempts have been made to estimate possible biomass in the European ocean based upon available carbon and flux rates, with a conclusion that the entire ocean may support as few as 10^{21} bacterial cells [9–11]. If they were homogeneously distributed, this would be < 1 cell/L.

The challenge of life detection on such a world is tremendous. Before we go to Europa, the challenge first is to develop methods that can detect prokaryotic life from any Earth environment, without underlying assumptions about chemical composition that may not be generalizable to life elsewhere.

Gold standards on Earth

For simple identification and enumeration of prokaryotes, without taxonomic classification, high-resolution light microscopic imaging is the tool of choice [12–14]. The key difference between microbial enumeration on Earth and extraterrestrial life detection is burden of proof. An error in microbial count of a factor of 2, or even 10, is unlikely to be critical in most terrestrial experiments. Claiming the existence of extraterrestrial life, on the other hand, will be subject to the world's skepticism. Prokaryotic cells do not have many features that distinguish them from debris (Figure 1(A) and (B)).

Simply increasing spatial resolution is not the answer. Even electron microscopy can be inconclusive in distinguishing prokaryotes from minerals, as exemplified by the ALH84001 meteorite controversy [15]. Definitive detection of microbial life requires several elements: context, chemical composition, and ideally activity of a sort consistent with life (growth, motility or cell division).

Meaningful motility can be an unambiguous sign of life, and requires less spatial resolution than recognition of single cells [16]. Brownian motion is readily distinguished from swimming or gliding. The mean-square displacement of a
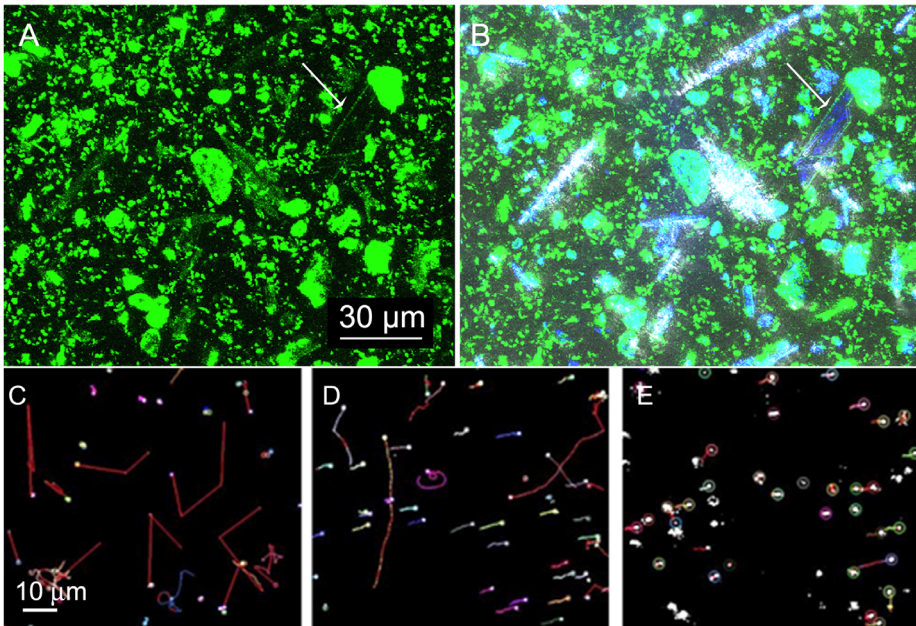
Figure 1. Identifying life with light microscopy. (A) A sample of dense biofilm containing cells and minerals, stained with the DNA-targeting dye SYTO9 and imaged with confocal microscopy. (A) With 488 nm excitation and 520 ± 20 nm bandpass emission, fluorescence is seen from a wide variety of objects which may or may not be cells. Some objects (arrow) do not bind dye and are clearly minerals, whereas some objects are ambiguous. (B) An overlay of reflectance on the fluorescence image helps to clarify which objects are highly reflective minerals. The objects that appear bright blue–white can be seen to correspond to little or no green fluorescence and are therefore minerals. The objects that appear turquoise remain ambiguous. (C) 10s tracks of motile organisms at their ideal temperature clearly shows multiple changes of direction inconsistent with drift or Brownian motion. (D) Cooling the sample creates some drift from left to right (due to thermally induced currents) and reduces the fraction of motile organisms, but some highly motile cells moving perpendicular to the drift can still be seen. (E) Past a critical temperature – which is highly strain-dependent – the cells stop swimming and only slight drift is apparent.

Brownian particle over time t is $x^2 = 2Dt$, where D is diffusivity. For a 1 μm sphere in water, this gives a displacement of 0.01 μm/s, compared with prokaryotic swimming speeds of 10–100 + μm/s. Brownian motion is also random and not directional, as opposed to swimming, which shows changes of direction. Such reversals also distinguish swimming from drift or flow (Figure 1(C)–(E)). A single motile organism is insufficient for life detection, but the appearance of multiple motile objects is compelling.

When organisms are non-motile, the existence of multiple cell-like structures with organic chemical composition is required to imply that life is present. Fluorescence microscopy can give that hint to composition. Fluorescence arises from autofluorescence or from selected tagging with dyes [17–19]. Autofluorescence is ubiquitous, representing pigments that serve diverse roles in bacterial autotrophy or protection from UV [20]; the most commonly considered as biosignatures are the photosynthetic pigments (chlorophylls) [21,22].

On the micrometer to centimeter scale, Raman spectroscopy and Fourier transform infrared spectroscopy (FTIR) have been shown to be useful for identifying pigment molecules in isolated cells, in environmental samples (minerals, rocks) containing micro-organisms, and in ancient rocks (Proterozoic to Paleozoic) [21,23–28]. These spectral signatures have also been suggested as targets for exoplanet investigations, using reflectance spectroscopy in the 0.35 to 1.2 μm wavelength range [29].

To obtain greater specificity for structural molecules particular to life and to increase the signal to noise, fluorescent dyes are used. Dyes can target nucleic acids (including nucleic acids not used in Earth life such as PNA [peptide nucleic acid] [30]); lipids, which are considered a likely universal biosignature [31]; and various other cell wall and membrane components. While these do imply some pre-supposition of extraterrestrial chemistry, the classes of molecules stained are broad enough that they are likely to exist on all water-based worlds. The most commonly used dyes show low background fluorescence, with a strong quantum yield increase upon binding to nucleic acids; DAPI and acridine orange are two such dyes. Fluorescence imaging increases the specific signal relative to the background, facilitating observation and counting and increasing effective spatial resolution.

The trade-offs with traditional optics between field of view, depth of field (dof), and spatial resolution (r) are all related to the numerical aperture (NA) of the objective lens used. Resolution is given by

$$r = \frac{0.61\lambda}{\text{NA}},$$

(1)

where λ is the wavelength of illumination, and dof is given by

$$\text{dof} = \frac{\lambda\sqrt{n^2 - \text{NA}^2}}{\text{NA}^2}$$

(2),

where n is the index of refraction of the imaging medium (1.0 for air and 1.33 for water).

Angle of view relates to NA simply as $\text{NA} = \sin\Theta$, where Θ is the half-angle of view of the system.

These values mean that for typical light microscopy at magnifications required to detect prokaryotes, the imaged volume is 10^{-4} μL or less. For microbial concentrations of 10^5–10^6 cells/mL, optimistic for Europa, this sampled volume represents significantly less than an average of one cell per image. All considerations of microscopic techniques for life detection must either increase throughput or pre-concentrate the samples by at least a hundredfold.

What this means for space

Non-microscopy techniques that have been suggested for life detection include the search for target organic molecules such as sugars and amino acids by mass spectrometry; spectral fingerprinting using Raman; evaluation of chirality of organic molecules, with the hypothesis that life will select for a single handedness; specific antibody arrays targeting key molecules; and culture-based methods [32–34]. However, by themselves, these chemical biosignatures will always be ambiguous. All the organic building blocks of life are known to be possible through abiotic origin and have been detected in interstellar space and/or in meteorites with no hint of biotic origin [35–37]. Homochirality, also, may be of abiotic origin [38,39].

Most importantly, if even the most robust chemical biosignatures are found in the absence of confirmed life, we can't be sure whether they are precursors to nascent life or molecular remnants of extinct life (or even both). If the goal is to look for extant life, then making this distinction is vital. The way life *looks, behaves, moves,* and *interacts with its environment* is the only way that we have of clearly distinguishing it from complex abiotic chemical reactions [40]. Science does not have a reductionist definition of life [41]. Even methods to detect active metabolism may be ambiguous, as evidenced by the on-going controversy regarding the Viking labeled release experiments [42]. A microscope on the Viking lander could have disambiguated those results [43].

Imaging for life detection

Despite its ubiquity on Earth, microscopy has been notably neglected in space flight instruments. Part of this is due to technical challenges; most microscopy techniques require expert manipulation and are sensitive to vibration and temperature extremes, and high-resolution microscopes are often large, heavy, and fragile. However, recent advances in microscopy have allowed for sub-micrometer resolution in compact, robust, autonomous instruments.

Direct imaging at larger spatial scales has been a part of virtually every planetary mission, using imagers designed for geology rather than microbiology such as the MAHLI hand lens [44,45]. Spectral characterization of minerals is performed in the infrared, with several miniature spectrometers proposed and selected for missions [46–49]. These instruments have been well reviewed elsewhere [50,46]. Here, we will focus specifically on what is needed for microbial life detection. We begin by defining specific needs of a microscope for life detection, then discuss microscopes that have flown. We then suggest some emerging imaging technologies appropriate for detection of microbial life on planetary missions, whether or not they have been proposed for flight.

Microscopes used on planetary missions

Some sophisticated microscopes have flown on the International Space Station (ISS), including a light microscopy module (LMM) [51] to which confocal and/or lifetime imaging performance is expected to be added. Both the European Space Agency (ESA) and the Japan Aerospace Exploration Agency (JAXA) have developed similar systems. These instruments and their applications have been well reviewed elsewhere [52], so in the interest of space we shall not discuss them here, but focus on instruments designed for autonomous operation in planetary missions.

The highest resolution optical microscope that has been selected for a Mars lander was on board the 2003 European Space Agency mission Beagle 2, which failed to land safely. The instrument was based upon a Cook triplet lens coupled to a fixed-focus monochromatic camera. Illumination was provided by LEDs of four colors (wavelengths for red, green, blue, and ultraviolet-A [373 nm]) [53]. Focusing was performed by translating the specimen along its axis in increments of the depth of field (40 µm). Algorithms for analyzing the successive focal planes have been developed [54]. The resolution was approximately 4 µm/pixel. This instrument has been used on Earth to investigate mineralized biosignatures [55].

Atomic force microscopy (AFM) can achieve sub-micrometer resolution with the robustness required for space. Invented in 1982, AFM is a type of scanning-probe microscopy in which a very fine tip is dragged across a surface (contact mode) or held close to surface without contact but with a controlled amplitude or frequency of vibration. A measurement of the tip-to-sample distance at each point provides an image. In vacuum it is usually frequency, rather than amplitude, which is modulated because the high Q-factor of cantilevers in vacuum makes amplitude control difficult. The first AFM designed for space was launched in 2004 but did not arrive at its target until 10 years later: this was the Micro-Imaging Dust Analysis System (MIDAS) AFM on the Rosetta mission, targeting Jupiter family comet 67P Churyumov–Gerasimenko. MIDAS's goal was to study the size, shape, and morphology of cometary dust particles with a spatial resolution of 4 nm, using both contact and non-contact mode (Figure 2(A)) [56]. Dust grains were collected by exposing sticky surfaces to the comet. Some images from MIDAS have been published; other data are currently being analyzed.

The second AFM launched for a space mission – but the first to arrive – was on the instrument called MECA (the Microscopy, Electrochemistry, and Conductivity Analyzer) on the Phoenix Mars lander (2007). The MECA AFM determined particle size distribution (PSD) of fines in the Martian regolith. It was coupled with an optical microscope with 4 µm/pixel that permitted higher resolution images of grains than previously obtained (Figure 2(B)–(D)) [57]. The optical microscope was used to locate particles in order to select areas for AFM imaging, an advantage that MIDAS did not have. Not knowing how much dust was collected presented a major challenge in determining how to scan with MIDAS.
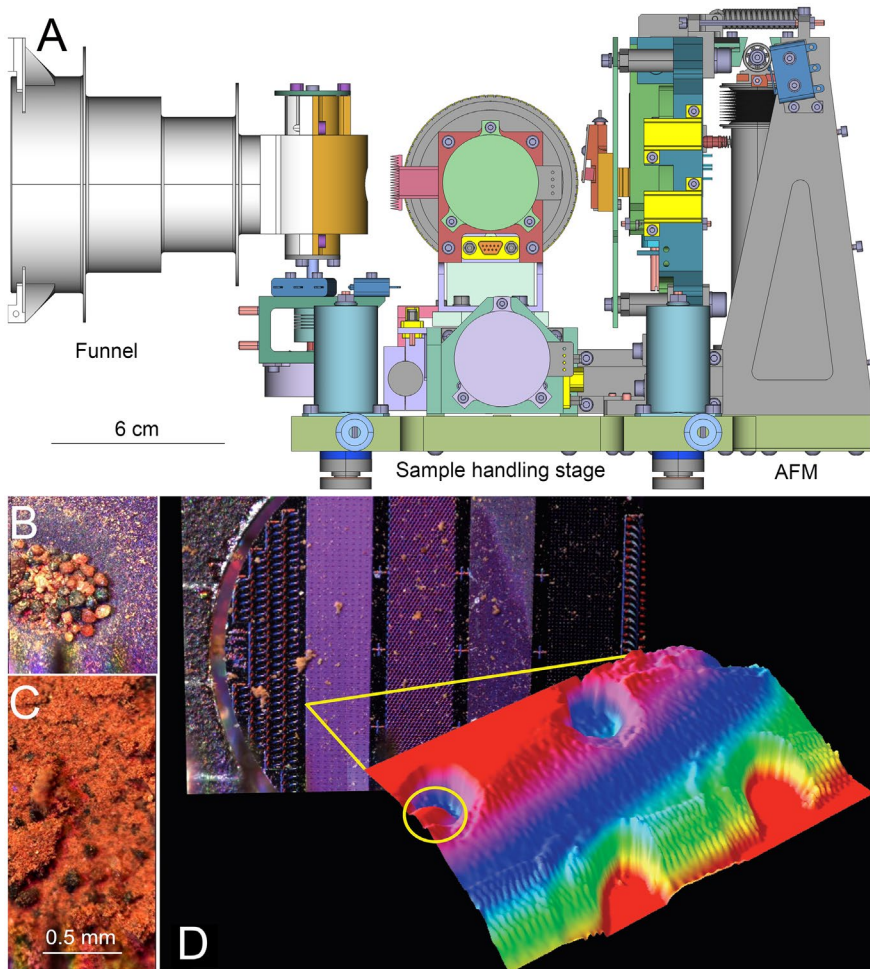
Figure 2. AFMs for flight. (A) Schematic of the MIDAS instrument showing the funnel for dust collection, sample handling stage, and the AFM (image courtesy M.S. Bentley). (B-D) Data from the optical microscope and AFM on MECA. (B, C) Fines imaged with the optical microscope. (D) An area of regolith identified by the optical microscope was selected and profiled with the AFM (image credit: NASA).

Table 1 summarizes the parameters of the microscopes that have flown on both successful and failed missions. While all of the instruments on successful missions worked as intended, it is important to note that they were intended as geological, not biological instruments. Detection of extant microbial life has somewhat different requirements than mineral characterization: higher spatial resolution (under a micrometer), ultraviolet or visible imaging rather than infrared, targeted labeling, high throughput, and ideally video. The report of the Europa lander science definition team (SDT) released in 2017 specifically identified a microscope as a key instrument for the first Europa lander, identifying desired performance parameters as defined in Table 2. How these parameters translate into microscope requirements for a potential Europa Lander mission is also given in Table 2 and more generally in [16].

Table 1. Microscopes that have flown on planetary missions.

Instrument name	Mission/year of launch	Type	Resolution	FOV	DOF	Illumination	Mass	Power
None	Beagle II (2003) (mission failed)	Optical/fluorescence	4 μm	4.2 × 4.2 mm	40 μm	RGB LEDs and UV	245 g	1.5 W
Athena Microimager	2003 (MER)	Optical/mono-chrome	30 μm	31 × 31 mm	3 mm	sunlight	290 g	4.3 W max/2.5 W typ
MIDAS*	Rosetta (2004)	AFM	Lateral:4 nm; height: 1 nm	100 μm × 100 μm max		–	8000 g	12 W avg
Optical microscope/ AFM[‡]	MECA (2007)	Brightfield AFM	4 μm 0.1 μm	1 mm × 2 mm 65 μm × 65 μm	50 μm 13 μm	RGB and UV LEDs –	Not available Not available	Not available Not available
PIXL MCC	Mars 2020 (NASA)	Optical	50 μm	37.6 mm × 29.1 mm		LED	361.5 g	4.31 W max
MicrOmega	ExoMars (2020?)	IR reflectance	20 μm	5 mm × 5 mm		0.9 to 3.5 μm in 500 channels		
SEMPA	Comet Rendezvous Asteroid Flyby (mission canceled)	SEM	40 nm			–	12 kg	22 W

*MIDAS imaging time is several hours/field.;
[‡]MECA imaging time is ~30 min/field.

Table 2. Microscope for Life Detection requirements transcribed from Europa the Europa Lander SDT report (Table 4.5.6). Numbering corresponds to the investigation numbering in the report. Investigation 1B3 is not included in the 'Threshold' mission concept. Translation into microscopic parameters is given in the third column.

Investigation	Measurement requirement	Microscope parameters
1B1. Resolve and Characterize microscale evidence for life in collected samples	Search for cells and other microstructures that are 0.2 micron or larger in their longest dimension	Spatial resolution of 0.2 micron or ability to track unresolved structures
1B3. Detect structural, compositional, or functional indicators of life	Measure structural, compositional, and/or functional properties such as biophysical or mechanical properties, native autofluorescence, or microspectroscopic signatures, associated with microscale particles in the sampled material	Ability to detect specific chemical signatures via fluorescence or spectral profiling in the UV, visible, and/or infrared.
3A1. Characterize the physical properties of Europa's surface materials through interaction with the sampling and landing systems	Measure physical and mechanical properties of surface 'fines' and regolith (i.e. loose, unconsolidated or weakly indurated fine-grained surface materials). Characterize textural and structural attributes of this material at millimeter scales in the workspace, and as exposed by the sample extraction tool. Measure physical and mechanical properties of solid surface materials (i.e. icy-shell material). Characterize textural and structural attributes of this material at millimeter-to-meter scales in the landing zone (~5 m)	Ability to image fines at micron-scale resolution, and to determine physical properties by different means (e.g. quantitative phase imaging, AFM tapping, dye binding)
3B2. Characterize the chemical processes that affect materials on Europa (e.g. radiolysis)	Characterize changes in ice and other surface materials in the landing zone (~5 m) in response to landing and sample collection, over mission duration (e.g. color, morphology, and composition)	RGB or full spectral capability coupled with micron-scale resolution

Emerging techniques of interest

Fluorescence microscopy

Fluorescence microscopy is universally used in studies of extraterrestrial analog samples such as sea ice, desert soils, and endolithic communities. Autofluorescence is nearly always too weak to be of value unless the organisms contain chlorophyll, which means dyes must be used; each environment requires special handling and staining considerations and an informed choice of dyes. For example, for *in situ* examination of frozen sea ice using DAPI, a higher concentration of the dye must be used than in room temperature experiments [58]. In samples from the ocean subfloor, HF may be used to eliminate mineral fluorescence and so increase the specific signal from the dyes [59]. All of these studies are of immense value in designing an extraterrestrial mission, as they will inform design of the hardware and protocols: choice of excitation/emission wavelengths, need for sample filtration/washing, and choice of imaging temperature.

A fluorescence microscope has not yet been used on another planet, but it is only a matter of time. A modified version of the Beagle 2 instrument was chosen for the ESA ExoMars 2018 mission, but this version will image in the infrared rather than the visible, specifically for characterizing mineral grains [60]. This instrument, called Micromega/IR, is part of the Pasteur payload with stated goals of looking for extant or extinct life. [61,62].

The Japanese space agency JAXA had been studying a mission concept for 2020 or 2022 launch called MELOS (Mars Exploration of Life-Organism Search). The mission included a rover carrying a fluorescence microscope, the LDM (Life Detection Microscope) [63]. Though the mission was not accepted for the launch window, the LDM team is continuing the development of the instrument. The goal will be to use the dyes SYTO24 and propidium iodide together. With this combination, organic compounds surrounded by lipid membranes will be green and those without membranes will be red; the former are most likely to be cells. Metabolic activity will be also detected by another dye, CFDA-AM, to confirm possible extant life forms. The team has demonstrated successful sample staining techniques in the Simulated Martian Soil JSC Mars-1. Not all details of the microscope design or dyes are available yet, but the target mass is 6 kg, power 20 W, and spatial resolution 1 μm. The limit of detection is ~10^4 cells/g of clay soil (Figure 3(A)).

The Biological Oxidant and Life Detection (BOLD) mission is a mission concept proposed in 2012. The general design involves six small probes capable of soft landing, each containing a life-detection or habitability–characterizing instrument. One of the proposed instruments is a microscope with the following characteristics: capable of both context imaging (~20 μm resolution) and high-resolution imaging (~1 μm); LED illumination with UV and red, green, and blue light; laser fluorescence excitation with labeling with three dyes (dyes not specified, but UV excitation is suggested); and possibly a spectrometer [64]. It is important to note
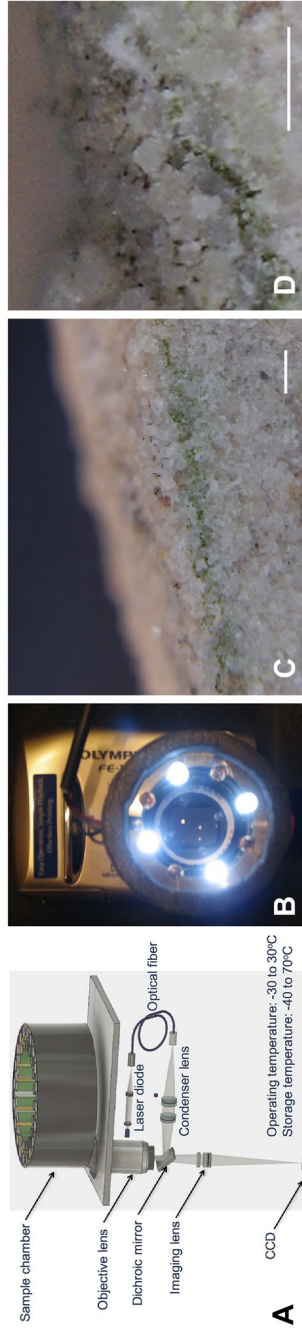
Figure 3. Fluorescence microscopes designed for planetary exploration. (A) Schematic of the JAXA LDM (image courtesy Akihiko Yamagishi). (B) Photograph of the multi-scale imager described in [65]. (C, D) Two images taken with the multi-scale imager of an endolithic microbial community; scale bar = 5 mm (images in B-D courtesy Wolfgang Fink).

that the microscope described is a concept only. However, several of the BOLD team have constructed a multiscale imager for astrobiology that incorporates many of the desired features, particularly the ability to image in context and then zoom in to 1.2 µm resolution [65] (Figure 3(B) and (C)).

The instruments for near-term missions will be based upon traditional optics, with objective lenses and probably moving parts such as turrets; mass will be on the order of 1–2 kg. However, significant miniaturization is possible based upon modern micro-electromechanical systems (MEMS) technology. Fluorescence microscopes have been made extremely small for biomedicine, where instruments have been made small enough to fit inside the brains of conscious mice. Illumination is by means of light-emitting diodes (LEDs) and the detector is a miniature CMOS. The entire package, not including computer, can be < 2.5 cm³ and weigh < 2 g [66].

Digital holographic microscopy (DHM)

Holography is an interferometric technique that encodes the electric field of a three-dimensional object as a pattern of fringes caused by the interference of a clean reference beam (R) with a beam that has passed through the object (O). A hologram is not an image; its intensity is given by a pattern of interference fringes given by:

$$
\begin{aligned}
I(x, y) &= \left| O(x, y) + R(x, y) \right|^2 \\
&= R(x, y)R^*(x, y) + O(x, y)O^*(x, y) + O(x, y)R^*(x, y) + R(x, y)O^*(x, y)
\end{aligned}
\tag{3},
$$

where * indicates the complex conjugate. Images can be reconstructed from the fringe pattern using some model assumptions, one of the most common of which is the Fresnel approximation; discussions of reconstruction methods are outside the scope of this article, but the reader is referred to several articles on the subject [67,68].

The use of holography has the immediate advantages of image compression and lack of need for focusing, both of which are important for space flight. A hologram may be reconstructed plane-by-plane into an intensity (bright-field) image and a quantitative phase image (Figure 4) [69,70].

A phase image is different from a Zernike phase contrast image; the phase shift is related to the optical path length (OPL) of the sample, which is a product of the refractive index difference between the cell (n_c) and the medium (n_m) and the cell thickness h:

$$
\Delta\varphi = \frac{2\pi}{\lambda} h(x, y) \left[n_c(x, y) - n_m \right]
\tag{4}.
$$

Using phase imaging allows for estimates of particle index of refraction if thickness can be determined independently – for example, using multiple wavelengths in
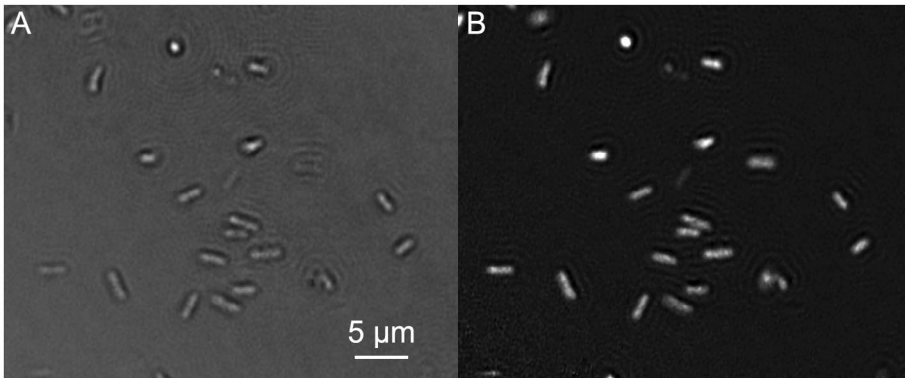
Figure 4. Amplitude and phase images of *E. coli* cells taken with the instrument described in [112]. (A) Amplitude image. (B) Phase image. Images were median subtracted to remove noise. Cells that appear out of focus on this plane may be reconstructed from the same hologram in focus on another *z* plane.

order to eliminate the *h* term in Equation (4), or altering the medium index in order to eliminate n_c [71,72].

Although usually performed with coherent light (lasers), ultra-compact DHMs can be made with incoherent illumination. DHM is diffraction-limited in the same way as imaging microscopes; breaking the diffraction limit has been demonstrated using structured illumination and other techniques, outside the scope of the discussion here, but the reader is referred to original papers on the topic [73–78].

DHM with coherent illumination

The advantage of coherent illumination is that the entire sample volume contributes to the recorded hologram, creating a large depth of field. A typical off-axis DHM is essentially a Mach Zehnder interferometer. Instruments with this design can achieve diffraction-limited resolution [79], but they are highly sensitive to misalignment and so less suitable for space flight. Several remedies have been proposed for this problem: robust packaging; common-path optics; and single-beam (in-line) designs.

- *Robust packaging*. A commercial instrument (LynceeTec, Switzerland) based upon a Mach–Zehnder design was packaged in a sturdy cage for parabolic aircraft flight [80] (Figure 5(A)). Such a design is suitable for aircraft use. The instrument contains multiple objective lenses and achieves sub-micrometer resolution.
- *Common-path optics*. We have reported a fieldable version of off-axis DHM that has a shared optical path for the object and reference beams (Figure 5(B)). This makes the interference fringes stable to vibration or shifts in alignment, since they will affect object beam and reference beam identically. This instrument has been successfully used to detect cells in Arctic sea ice brines and desert springs, demonstrating a limit of detection of $\sim 10^4$

organisms mL^{-1} in a single 0.25 μL sample without sample pre-concentration [81,82].

- *Digital in-line holographic microscopy (DIHM)*. Holographic microscopy on dilute samples may be performed with only a single beam that serves as its own reference, with the deviation caused by the sample considered as a perturbation (Figure 5(C)). This configuration imposes additional complications on the reconstruction, but rapid algorithms have been developed for this [83]. At least two commercial DIHMs have been developed for submersible use and used to image plankton and particulate matter. One is commercially available from 4-Deep [84,85] and another from Sequoia Scientific [86,87]. Spatial resolution of these in-line instruments is insufficient for prokaryotes; on the other hand, their sample volumes are very large (50 mm deep).
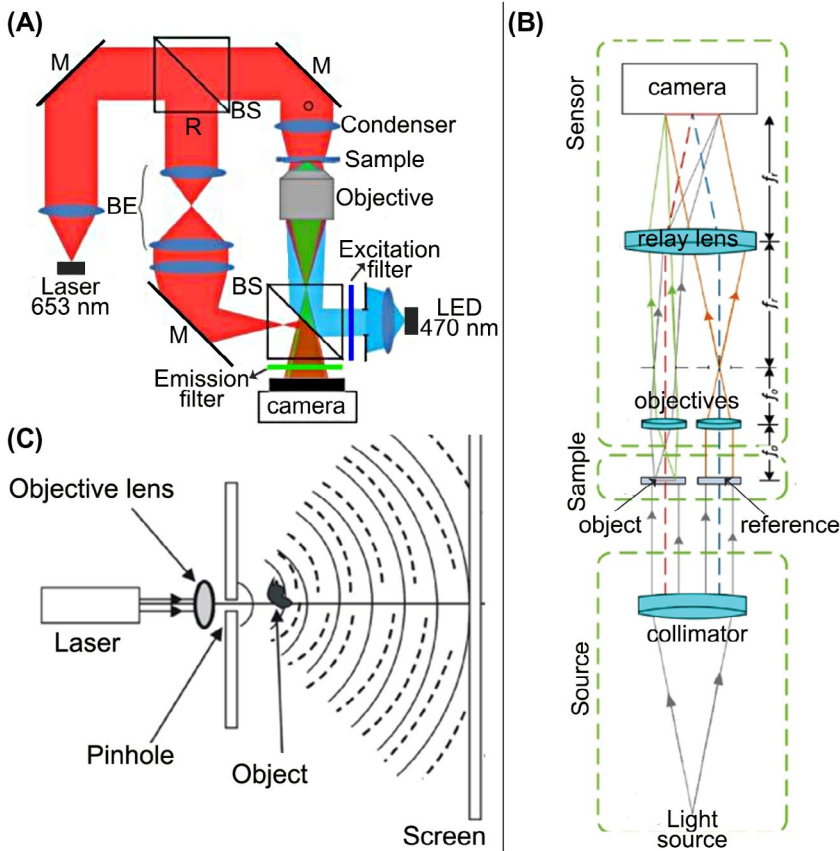

Figure 5. Designs of robust DHM instruments. (A) Mach–Zehnder design with added fluorescence capability, as packaged into an instrument for parabolic flight (from [113], used with permission). (B) 'Common-mode' design as in [114], where all mechanical and thermal perturbations will be seen equally by both the object and reference beam. (C) In-line, single-beam design as in [84].

DHM with incoherent illumination

Extremely small, robust, low-power microscopes have been constructed using light-emitting diodes in an in-line DIHM geometry. This type of design is lensless and may be coupled to microfluidics to create compact on-chip systems. The advantages of this approach are very low mass and low power, insensitivity to alignment, and lack of mechanically sensitive optics. Field of view is also decoupled from resolution because there is no objective lens. The field of view is 24 mm² without scanning and the entire instrument weighs < 100 g (Figure 6). Super-resolution has been achieved in these systems using LEDs arrays where each is sequentially illuminated [88] and a corresponding frame of data captured. In this case, the image from each LED is a slightly shifted hologram; the Fourier representations may be summed to achieve ~800 nm spatial resolution.
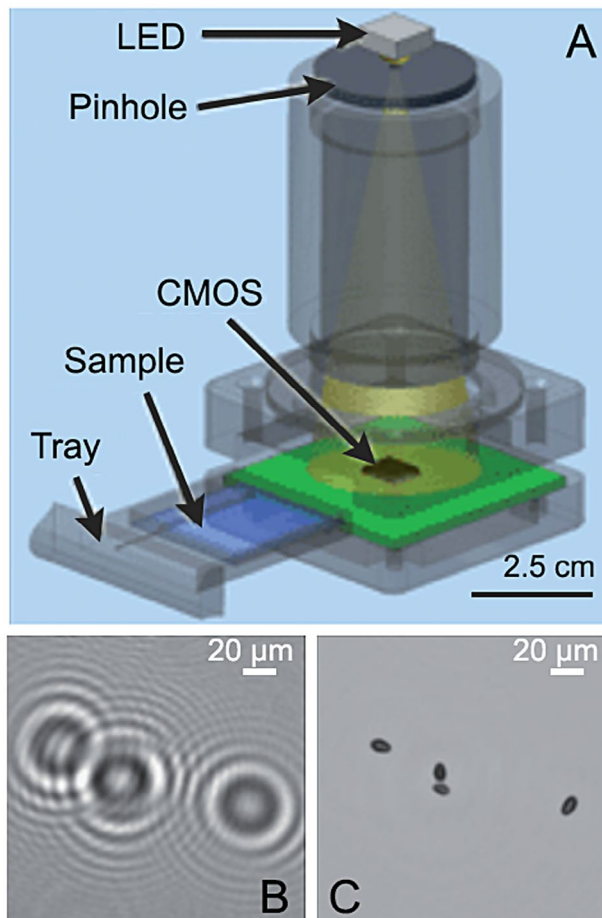

Figure 6. Ultracompact lensless DHM. (A) Image schematic showing integration with on-chip camera and sample tray. (B) Raw holograms of *Giardia lamblia* cysts. (C) Amplitude reconstruction of holograms at best focus (From: [115], used with permission).

The drawbacks are low depth of field relative to coherent-light DHM and the inability to image fast motion if sequential illumination is used. The proximity of the sample to the detector can also expose the sample to undesired heating from the detector. These instruments are ideal for samples that are large and flat – for example, cultured cells. The addition of RGB capability permits real-color imaging of stains or other features [89–92].

Other very small lensless microscopes, which are not holographic, have been described in the literature. These may be based upon shadow imaging, with spatial resolution limited by diffraction of the emitted light over the distance between the sample and sensor (usually on the order of 100 μm). These have been well reviewed elsewhere [93].

Imaging flow cytometry

In Earth oceans, submersible microscopes have been designed for detailed characterization of phytoplankton. Different instruments have been designed for different spatial scales. At scales > 100 μm, there are multiple instruments which have been reviewed elsewhere [94]. Fewer instruments exist to look at smaller cells. The FlowCytobot is designed to sample cells at 1–10 μm, using flow cytometry but not imaging. The Imaging FlowCytobot takes pictures of cells in the size range 10–100 μm [95], passing one cell at a time through a flow cell tens of μm deep in order to keep the cells in focus. The Imaging FlowCytobot is able to detect all of the cells seen by a commercial, non-imaging cytometer, and more cells than found by an expert microscopist. Imaging may be triggered by chlorophyll fluorescence or by scattering indicating a particle. The use of chlorophyll is quite specific for living cells; the use of scattering as a trigger results in imaging some empty diatom frustules and other debris. The quality of the images is spectacular when gated on chlorophyll (Figure 7).

The limitations to throughput in this type of instrument are mostly due to blur (motion blur and out-of-focus blur). Improvements can be realized using light-sheet illumination, as reported in [96]. This allows for throughput of ~1 mL/min with spatial resolution of ~1 μm. Another method is to use acoustic focusing (H. Sosik, submitted).

These instruments are designed for Earth use and so have not been miniaturized. The FlowCytobot uses 100 W of power and weighs tens of kg; the Imaging FlowCytobot is commercially available from McLane Laboratories, which reports power usage of 35 and a mass of 32 kg, with neutral buoyancy. A highly miniaturized instrument has not yet been developed for space flight, though no insurmountable barriers to miniaturization exist. Because the instruments operate autonomously in the ocean, the lessons learned about sample processing, *in situ* cleaning, and length of useful operation would be invaluable to mission design. A review of existing instruments and their performance may be found in [97].
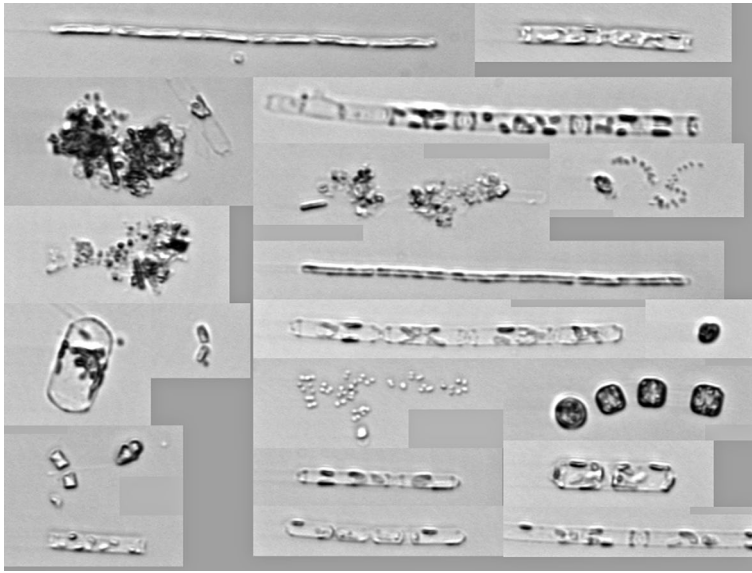
Figure 7. An example of images from the Imaging FlowCytobot. Image taken from the public data repository at http://ifcb-data.whoi.edu/mvco.

Electron microscopy

Electron microscopy (EM) – both scanning (SEM) and transmission (TEM) – is widely used by both geologists and biologists. 'Environmental' SEM permits samples to be held under low-pressure water vapor, usually ~8 mbar, which is sufficient for imaging live cells. Energy-dispersive X-ray spectroscopy (EDS) is often coupled with EM to provide elemental composition information about a sample. The combination of the high resolution attainable using electrons (tens of nm) and the elemental information allows for analysis of composition of minerals, including biogenic minerals, calculation of particle size distributions and morphologies, and identification of nanoscale cellular features such as flagella and pili. Sample throughput is a major drawback of electron microscopy – the imaged volume is so small that it would not be useful for the 'search' part of a life detection instrument, though if candidate objects could be identified and brought into the field of the EM it could be valuable for evaluation of features indicative of life.

The difficulty in miniaturizing EM for space flight lies in the size of the electron gun (often hundreds of kg) and the power required to accelerate the electrons (kW). The electron beam must be powerful enough to generate enough x-rays for EDS.

Despite the challenges, compact SEMs have been built and flight qualified as early as the 1980s. The SEM and Particle Analyzer (SEMPA) included SEM and EDS and had ~40 μm spatial resolution with a 12 kg/22 W payload [98]. It was designed for the Comet Rendezvous Asteroid Flyby, which was canceled.

Since then, further developments in electron optics and silicon microfabrication have permitted greater resolution and miniaturization. A miniaturized environmental scanning electron microscope (ESEM) was developed specifically for lunar exploration, where ambient vacuum obviates the need for a vacuum chamber. The same group later added variable-pressure capability with Mars exploration in mind [99]. Either of these designs is appropriate for use on outer planet moons.

Lightfield microscopy

Lightfield microscopy uses a lenslet array inserted into the intermediate image plane of a conventional microscope, allowing three-dimensional information to be collected from the sample by measuring the local intensities of the light field. This three-dimensional information must be extracted from the raw light-field image by means of digital processing.

The experimental setup of light-field microscopy is similar to that of conventional microscopy with the exception of the lenslet array. The sensor is then placed one focal length away from the lenslet array. Incoming light is focused onto the sensor and can be used to digitally analyze the incoming lightfield wavefront as opposed to only the light-field intensity [100]. A prototype light-field instrument that achieves a lateral resolution of 3.1 micrometers and an axial resolution on the order of tens of micrometers was reported in 2006 [101] (Figure 8). Since then, progress has been made in both hardware and image processing.

Once a light field is recorded by the sensor, it must be digitally processed in order to yield usable 3D information. It has been well established that the image reconstruction process of a light field image is very similar to the reconstruction of a tomographic image [102–104]. Thus, by analyzing one pixel from each subimage in the light field image, it is possible to create multiple perspective views of the object in the image. These perspective views can be used to create an image stack of the volumetric object. By the Fourier Slice Theorem, these perspective views can be combined to reconstruct the volumetric object (O) by the deconvolution of the image stack with the point spread function (PSF) of the optical system:

$$O = \mathfrak{F}^{-1}\left(\frac{\mathfrak{F}(F_S)}{\mathfrak{F}(P_{SF})} \right) \tag{5}$$

where $\mathfrak{F}$ is the Fourier Transform operator, $\mathfrak{F}^{-1}$ is the inverse Fourier Transform, F_S is the image stack obtained from the various perspective views of the object, and P_{SF} is the point spread function of the optical system. The PSF is generally measured empirically by the imaging of an unresolved fluorescent bead, analogous to the impulse response of the instrument.

This technique is valid on microscales where the object being reconstructed is relatively transparent and so the recorded light field is a result of the projection of light through and around the object, and not as a result of scattering. Functional
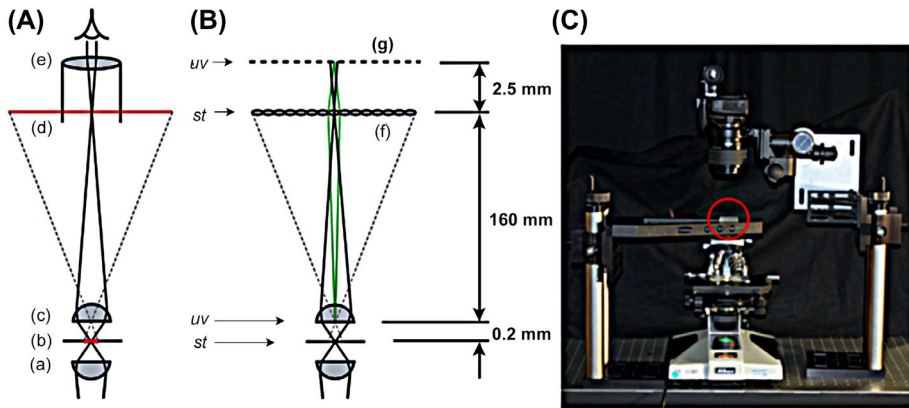
Figure 8. Light-field microscopy. (A) Optical schematic of an ordinary transmission-mode microscope. An illumination source is focused by a condenser lens at (a) onto a specimen at (b). An objective lens at (c) magnifies the specimen, creating a real image at intermediate image plane (d). In older microscopes, this plane is located inside the microscope tube. An ocular (eyepiece) at (e) further magnifies the central portion of this image, creating a second image focused at infinity. (B) Light-field microscope. The ocular is removed, a microlens array (f) is placed at the intermediate image plane, and a camera sensor is placed behind this at (g), positioned so that each microlens records an in-focus image of the objective (rays). In light-field parlance, if the objective aperture and specimen constitute the *uv* and *st* planes, then the camera sensor and microlens array constitute a reimaging of these two planes. This drawing is not to scale; typical distances are shown beside it (Figure courtesy Marc Levoy). (C) Photo of instrument.

imaging may be obtained by the use of dyes as markers for certain molecules or processes of interest.

Other image reconstruction algorithms have been reported and extensively studied but rely on iterative processes that are very computationally demanding relative to the deconvolution method [105].

Fourier Ptychographic Microscopy

Fourier Ptychographic Microscopy [106] (FPM) is a recently developed synthetic-aperture imaging technique that enables imaging at resolutions higher than the diffraction limit of the imaging optics. FPM achieves this by recording multiple images of the object of interest with illumination provided from a point source at a different angle for each image (Figure 9). High-resolution images are then obtained by a combination of phase retrieval and iterative combination of the intensity images, the phase information, and the optical system characteristics to obtain self-consistent solutions for the complex light field at the sample. This ability to retrieve both the phase and amplitude of the light gives FPM quantitative phase-imaging capabilities similar to DHM. Although FPM does not directly improve fluorescence imaging because the angle of the fluorescing object into the optical system is fixed, the FPM process provides detailed information about optical system aberrations that can be used to improve fluorescence image quality by removing those aberrations [107].
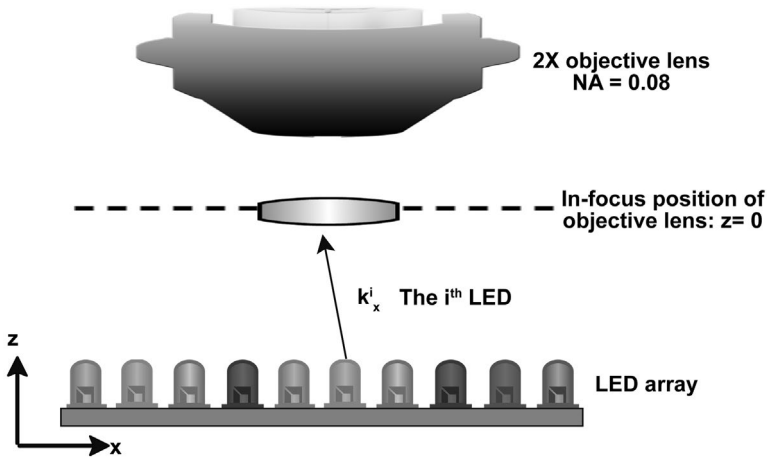
Figure 9. FPM. FPM uses a 2D array of light sources (LEDs in this image) to record multiple low-resolution images that can be stitched together to form a much higher resolution image than the imaging system NA supports.

In the laboratory, FPM can be performed using a conventional microscope using a special illuminator array. The depth of field and field of view of the system remain the same as those of the imaging optics, but the effective NA that defines the resolution of the system is the sum of the NA of the imaging optics and the NA of the illumination array. This allows for very high NA (>1) microscopy with a large field of view, making it very appealing for use in planetary missions. Depth of focus of the system is typically ~25× larger than would be achieved in a system with a similar NA on the imaging optics, an additional advantage over conventional imaging. The illuminator array provides some redundancy – loss of a small number of the point sources results in only a small loss in the imaging capability.

The high-resolution image retrieval process for FPM offers both advantages and drawbacks for space missions. To synthesize high-resolution images, FPM uses a phase retrieval process that uses the small shifts in illumination angle provided by the multiple point sources to extract phase information about the light field from the set of images. It is similarly to ptychography that has been used in X-ray and electron microscopy, but the FPM process is done primarily using Fourier transformed images. The extraction of phase and amplitude information from the image set allows for calculation of images over a large volume, similar to holography, and also enables computational correction of aberrations in the optical system. The corrections can be applied both in the FPM images, and in conventional images taken with the same optics but without the FPM illumination and reconstruction process. After retrieval of the high-resolution image information, the original low-resolution images can be discarded, leaving ~10% of the original data volume. The main drawback is the computation resources required, approximately 10 min on a modern laptop without a GPU [106], which may still be 100s of times faster

than a typical spacecraft computer. The data volume vs. computing requirements trade would need to be done for specific mission applications.

Multimodal optical sensing

Many of the optical imaging systems described above are compatible with each other in that minor modifications to the optics (e.g. addition of a beamsplitter and relay mirror) can enable more than one imaging mode simultaneously or on the same sample volume. Some multi-modal instruments have already been constructed – e.g. the MECA OM/AFM allowed AFM imaging of a small area of the OM field, and integration of FPM and AFM has been demonstrated in the laboratory [107,108]. The MIDAS team highlighted the value that addition of an optical microscope would have provided in knowing whether sample had been collected and where in the field it was located [56]. An ideal system might have imaging at several scales and wavelengths combined in order to distinguish minerals (interesting at IR wavelengths) from biological materials (possibly more interesting at shorter wavelengths and with fluorescent dyes applied). AFM can be used both for very high-resolution imaging and as a mechanical probe to distinguish vesicles from mineral grains by their mechanical properties [109]. Stimuli can also be incorporated to determine if cell-like objects display taxis.

Summary and conclusion

Despite its universality for both mineralogical and microbiological applications on earth, microscopy has been neglected on landed missions to other planets. With increased interest in detection of extant microbial life, particularly on Europa, this is likely to change soon, but the parameters of the ideal microscope for space applications remain to be defined.

Even the best optical instrument will likely need to be coupled to additional instruments to eliminate ambiguity or – in the best-case scenario – begin to explore the biochemistry of extraterrestrial life. Measurements of metabolism to determine amino acid and sugar preferences and composition, acoustic measurements, and mass spectrometry would all be valuable complements to an imaging system.

For extension of the discussion of extant life to extinct or fossilized life, the situation becomes even more complex. Minerals can self-organize into biomimetic shapes [110], so morphology alone is insufficient as a biosignature. Recent studies in Antarctica have shown that no single instrument provided unambiguous results on a mummified microbial mat unless the exact biochemistry was known, permitting sequencing or antibodies to be used [111]. Further Earth-based studies are needed to define a suite of instruments that strikes a balance between pre-supposition of composition and ability to distinguish life from non-life.

Disclosure statement

No potential conflict of interest was reported by the authors.

Funding

References

[1] A.F. Davila, M. Skidmore, A.G. Fairen, C. Cockell and D. Schulze-Makuch, Astrobiology 10 (2010) p.705.

[2] F.J. Martin-Torres, M.-P. Zorzano, P. Valentin-Serrano, A.-M. Harri, M. Genzer, O. Kemppinen, E.G. Rivera-Valentin, I. Jun, J. Wray, M. Bo Madsen, W. Goetz, A.S. McEwen, C. Hardgrove, N. Renno, V.F. Chevrier, M. Mischna, R. Navarro-Gonzalez, J. Martinez-Frias, P. Conrad, T. McConnochie, C. Cockell, G. Berger, A.R. Vasavada, D. Sumner and D. Vaniman, Nat. Geosci. 8 (2015) p.357.

[3] D.C. Fernandez-Remolar, O. Prieto-Ballesteros, N. Rodriguez, F. Gomez, R. Amils, J. Gomez-Elvira and C.R. Stoker, Astrobiology 8 (2008) p.1023.

[4] R.L. Mickol and T.A. Kral, Orig. Life. Evol. Biosph. 47 (2016) p.511.

[5] C. Cousins, Astron Geophys. 52 (2011) p.36.

[6] P.J. Boston, L.D. Hose, D.E. Northup and M.N. Spilde, Geol. Soc. Am. Spec. Pap. 404 (2006) p.331.

[7] N. Sinha, S. Nepal, T. Kral and P. Kumar, Planet. Space Sci. 136 (2017) p.15.

[8] J. Saur, S. Duling, L. Roth, X. Jia, D.F. Strobel, P.D. Feldman, U.R. Christensen, K.D. Retherford, M.A. McGrath, F. Musacchio, A. Wennmacher, F.M. Neubauer, S. Simon and O. Hartkorn, J. Geophys. Research-Space Phys. 120 (2015) p.1715.

[9] C.F. Chyba and K.P. Hand, Science 292 (2001) p.2026.

[10] K.P. Hand, R.W. Carlson and C.F. Chyba, Astrobiology 7 (2007) p.1006.

[11] K.P. Hand, C.F. Chyba, R.W. Carlson and J.F. Cooper, Astrobiology 6 (2006) p.463.

[12] K. Porter and Y. Feig, Limnol. Oceanogr. 25 (1980) p.943.

[13] R.L. Kepner Jr and J.R. Pratt, Microbiol. Rev. 58 (1994) p.603.

[14] Y. Kawasaki, Adv. Space Res. 23 (1999) p.309.

[15] K.L. Thomas-Keprta, S.J. Clemett, D.A. Bazylinski, J.L. Kirschvink, D.S. McKay, S.J. Wentworth, H. Vali E.K. Gibson Jr and C.S. Romanek, Appl. Environ. Microbiol. 68 (2002) p.3663.

[16] J. Nadeau, C. Lindensmith, J.W. Deming, V.I. Fernandez and R. Stocker, Astrobio. 16 (2016) p.755.

[17] Y. Kawasaki, *Direct detection of Martian microorganisms based on fluorescence microscopy*, in *Life Sciences: Exobiology*, 1999, p. 309.

[18] K.G. Porter and Y.S. Feig, Limnol. Oceanogr. 25 (1980) p.943.

[19] R.L. Kepner and J.R. Pratt, Microbiol. Rev. 58 (1994) p.603.

[20] S. Abyzov, *Microorganisms in the Antarctic ice*, in *Antarctic Microbiology*, E. Friedmann, ed., Wiley-Liss Inc, New York, 1993, p.265.

[21] J.M. Stromberg, D.M. Applin, E.A. Cloutis, M. Rice, G. Berard and P. Mann, Int. J. Astrobiol. 13 (2014) p.203.

[22] S. Seager, E.L. Turner, J. Schafer and E.B. Ford, Astrobiology 5 (2005) p.372.

[23] Y.D. Winters, T.K. Lowenstein and M.N. Timofeeff, Astrobiology 13 (2013) p.1065.

[24] L.R. Dartnell, K. Page, S.E. Jorge-Villar, G. Wright, T. Munshi, I.J. Scowen, J.M. Ward and H.G.M. Edwards, Anal. Bioanal. Chem. 403 (2012) p.131.

[25] H.G.M. Edwards, I.B. Hutchinson, R. Ingley, J. Parnell, P. Vitek and J. Jehlicka, Astrobiology 13 (2013) p.543.

[26] J. Jehlicka, H.G.M. Edwards and A. Orenc, Appl. Environ. Microbiol. 80 (2014) p.3286.

[27] D.E.G. Briggs and R.E. Summons, BioEssays 36 (2014) p.482.

[28] L.J. Preston, D. Johnson, C.S. Cockell and M.M. Grady, Appl. Spectrosc. 69 (2015) p.1059.

[29] E.W. Schwieterman, C.S. Cockell and V.S. Meadows, Astrobiology 15 (2015) p.341.

[30] G. Manzini, M.L. Barcellona, M. Avitabile and F. Quadrifoglio, Nucleic Acids Res. 11 (1983) p.8861.

[31] C.D. Georgiou and D.W. Deamer, Astrobiology 14 (2014) p.541.

[32] R.E. Summons, P. Albrecht, G. McDonald and J.M. Moldowan, Space Sci. Rev. 135 (2008) p.133.

[33] H.G.M. Edwards, I.B. Hutchinson and R. Ingley, Int. J. Astrobiol. 11 (2012) p.269.

[34] O. Prieto-Ballesteros, E. Vorobyova, V. Parro, J.A.R. Manfredi and F. Gomez, Adv. Space Res. 48 (2011) p.678.

[35] A. Belloche, H.S.P. Mueller, K.M. Menten, P. Schilke and C. Comito, Astron. Astrophys. 559 (2013) p.A47.

[36] S. Kwok, Astron. Astrophys. Rev. 24 (2016) p.8.

[37] P. Theule, F. Duvernay, G. Danger, F. Borget, J.B. Bossa, V. Vinogradoff, F. Mispelaer and T. Chiavassa, Adv. Space Res. 52 (2013) p.1567.

[38] P. Cintas and C. Viedma, Chirality 24 (2012) p.894.

[39] G. Cooper and A.C. Rios, Proc. Natl. Acad. Sci. U. S. A. 113 (2016) p.E3322.

[40] C.P. McKay, Plos Biol. 2 (2004) p.1260.

[41] C.E. Cleland and C.F. Chyba, Origins Life Evol. Biosphere 32 (2002) p.387.

[42] G. Biancardi, J.D. Miller, P.A. Straat and G.V. Levin, Int. J. Aeronaut. Space Sci. 13 (2012) p.14.

[43] G.V. Levin and P.A. Straat, Astrobiology 16 (2016) p.798.

[44] K.S. Edgett, R.A. Yingst, M.A. Ravine, M.A. Caplinger, J.N. Maki, F.T. Ghaemi, J. Schaffner, J.F. Bell, L.J. Edwards, K.E. Herkenhoff, E. Heydari, L.C. Kah, M.T. Lemmon, M.E. Minitti, T.S. Olson, T.J. Parker, S.K. Rowland, J. Schieber, R.J. Sullivan, D.Y. Sumner, P.C. Thomas, E.H. Jensen, J.J. Simmonds, A.J. Sengstacken, R.G. Willson and W. Goetz, Space Sci. Rev. 170 (2012) p.259.

[45] R.A. Yingst, K.S. Edgett, M.R. Kennedy, G.M. Krezoski, M.J. McBride, M.E. Minitti, M.A. Ravine and R.M.E. Williams, Geosci. Instrum. Meth. 5 (2016) p.205.

[46] J.I. Nunez, J.D. Farmer, R.G. Sellar, G.A. Swayze and D.L. Blaney, Astrobiology 14 (2014) p.132.

[47] R.C. Wiens, S. Maurice and F.R. Perez, Spectroscopy-Us 32 (2017) p.50.

[48] P.R. Christensen, M.B. Wyatt, T.D. Glotch, A.D. Rogers, S. Anwar, R.E. Arvidson, J.L. Bandfield, D.L. Blaney, C. Budney, W.M. Calvin, A. Faracaro, R.L. Fergason, N. Gorelick, T.G. Graff, V.E. Hamilton, A.G. Hayes, J.R. Johnson, A.T. Knudson, H.Y. McSween, G.L. Mehall, L.K. Mehall, J.E. Moersch, R.V. Morris, M.D. Smith, S.W. Squyres, S.W. Ruff and M.J. Wolff, Science 306 (2004) p.1733.

[49] M.D. Smith, M.J. Wolff, N. Spanovich, A. Ghosh, D. Banfield, P.R. Christensen, G.A. Landis and S.W. Squyres, J. Geophys. Research-Planets 111 (2006) p.E12S13.

[50] M.D. Gunn and C.R. Cousins, Earth Space Sci. 3 (2016) p.144.

[51] C.T. Lant and A. Resnick, Aip Conf. Proc. 504 (2000) p.324.

[52] W.H. De Vos, D. Beghuin, C.J. Schwarz, D.B. Jones, J.J.W.A. van Loon, J. Bereiter-Hahn and E.H.K. Stelzer, Rev. Sci. Instrum. 85 (2014) p.101101.

[53] N. Thomas, B.S. Luthi, S.F. Hviid, H.U. Keller, W.J. Markiewcz, T. Blumchen, A.T. Basilevsky, P.H. Smith, R. Tanner, C. Oquest, R. Reynolds, J.L. Josset, S. Beauvivre, B. Hofmann, P. Ruffer and C.T. Pillinger, Planet. Space Sci. 52 (2004) p.853.

[54] B.S. Luethi, N. Thomas, S.F. Hviid and P. Rueffer, Planet. Space Sci. 58 (2010) p.1258.

[55] D. Pullan, F. Westall, B.A. Hofmann, J. Parnell, C.S. Cockell, H.G.M. Edwards, S.E.J. Villar, C. Schroeder, G. Cressey, L. Marinangeli, L. Richter and G. Klingelhoefer, Astrobiology 8 (2008) p.119.

[56] M.S. Bentley, H. Arends, B. Butler, J. Gavira, H. Jeszenszky, T. Mannel, J. Romstedt, R. Schmied and K. Torkar, Acta Astronaut. 125 (2016) p.11.

[57] W.T. Pike, U. Staufer, M.H. Hecht, W. Goetz, D. Parrat, H. Sykulska-Lawrence, S. Vijendran and M.B. Madsen, Geophys. Res. Lett. 38 (2011) p.L24201.

[58] K. Junge, C. Krembs, J. Deming, A. Stierle and H. Eicken, Ann. Glaciol. 33 (2001) p.304.

[59] Y. Morono, T. Terada, N. Masui and F. Inagaki, ISME J. 3 (2009) p.503.

[60] V. Leroi, J.P. Bibring and M. Berthe, Planet Space Sci. 57 (2009) p.1068.

[61] N. Bost, C. Ramboz, N. LeBreton, F. Foucher, G. Lopez-Reyes, S. De Angelis, M. Josset, G. Venegas, A. Sanz-Arranz, F. Rull, J. Medina, J.L. Josset, A. Souchon, E. Ammannito, M.C. De Sanctis, T. Di Iorio, C. Carli, J.L. Vago and F. Westall, Planet. Space Sci. 108 (2015) p.87.

[62] D. Barnes, E. Battistelli, R. Bertrand, F. Butera, R. Chatila, A. Del Biancio, C. Draper, A. Ellery, R. Gelmi, F. Ingrand, C. Koeck, S. Lacroix, P. Lamon, C. Lee, P. Magnani, N. Patel, C. Pompei, E. Re, L. Richter, M. Rowe, R. Siegwart, R. Slade, M.F. Smith, G. Terrien, R. Wall, R. Ward, L. Waugh, M. Woods and R. Team, Int. J. Astrobiol. 5 (2006) p.221.

[63] A. Yamagishi, S.I. Yokobori, Y. Yoshimura, M. Yamashita, H. Hashimoto, T. Kubota, H. Yano, J. Haruyama, M. Tabata, K. Kobayashi, H. Honda, Y. Utsumi, T. Itoh, K. Hamase, T. Naganuma, S. Sasaki and H. Miyamoto, Paleontol. J. 46 (2012) p.1087.

[64] D. Schulze-Makuch, J.N. Head, J.M. Houtkooper, M. Knoblauch, R. Furfaro, W. Fink, A.G. Fairen, H. Vali, S.K. Sears, M. Daly, D. Deamer, H. Schmidt, A.R. Hawkins, H.J. Sun, D.S.S. Lim, J. Dohm, L.N. Irwin, A.F. Davila, A. Mendez and D. Andersen, Planet. Space Sci. 67 (2012) p.57.

[65] W. Fink, H.J. Sun, W.C. Mahaney, K.R. Kuhlman and D. Schulze-Makuch, Astrobiology 13 (2013) p.1005.

[66] K.K. Ghosh, L.D. Burns, E.D. Cocker, A. Nimmerjahn, Y. Ziv, A.E. Gamal and M.J. Schnitzer, Nature Methods 8 (2011) p.871.

[67] J. Pomarico, U. Schnars, H.J. Hartmann and W. Juptner, Appl. Opt. 34 (1995) p.8095.

[68] C. Knox, Science 153 (1966) p.989.

[69] C. Mann, L. Yu, C.M. Lo and M. Kim, Opt. Express 13 (2005) p.8693.

[70] P. Marquet, B. Rappaz, P.J. Magistretti, E. Cuche, Y. Emery, T. Colomb and C. Depeursinge, Opt. Lett. 30 (2005) p.468.

[71] B. Rappaz, P. Marquet, E. Cuche, Y. Emery, C. Depeursinge and P. Magistretti, Opt. Express 13 (2005) p.9361.

[72] B. Rappaz, F. Charriere, C. Depeursinge, P.J. Magistretti and P. Marquet, Opt. Lett. 33 (2008) p.744.

[73] V. Mico, Z. Zalevsky, C. Ferreira and J. Garcia, Opt. Express 16 (2008) p.19260.

[74] V. Mico, Z. Zalevsky and J. Garcia, Optics Communications 281 (2008) p.4273.

[75] G. Brooker, N. Siegel, J. Rosen, N. Hashimoto, M. Kurihara and A. Tanabe, Opt. Lett. 38 (2013) p.5264.

[76] W. Luo, Z. Gorocs, Y.B. Zhang, A. Feizi, A. Greenbaum and A. Ozcan, Optics and Biophotonics in Low-Resource Settings Ii 9699 (2016).

[77] A.H. Phan, J.H. Park and N. Kim, Jpn. J. Appl. Phys. 50 (2011) p.092503.

[78] A.H. Phan, J.H. Park, N. Kim and S.H. Jeon, Pract. Hologr. Xxiv: Mater. Appl. 7619 (2010) p.UNSP 76190Q.

[79] J. Kuhn, B. Niraula, K. Liewer, J.K. Wallace, E. Serabyn, E. Graff, C. Lindensmith and J.L. Nadeau, Rev. Sci. Instruments 85 (2014) p.123113.

[80] M.F. Toy, S. Richard, J. Kuehn, A. Franco-Obregon, M. Egli and C. Depeursinge, Biomed. Opt. Express 3 (2012) p.313.

[81] C.A. Lindensmith, S. Rider, M. Bedrossian, J.K. Wallace, E. Serabyn, G.M. Showalter, J.W. Deming and J.L. Nadeau, Plos One 11 (2016) p.e0147700.

[82] M. Bedrossian, C. Lindensmith and J. Nadeau, Astrobiology 17 (2017) p.913.

[83] M. Kanka, R. Riesenberg and H.J. Kreuzer, Opt. Lett. 34 (2009) p.1162.

[84] S.K. Jericho, P. Klages, J. Nadeau, E.M. Dumas, M.H. Jericho and H.J. Kreuzer, Planet. Space Sci. 58 (2010) p.701.

[85] N.I. Lewis, W.B. Xu, S.K. Jericho, H.J. Kreuzer, M.H. Jericho and A.D. Cembella, Phycologia 45 (2006) p.61.

[86] H.K. Ha, Y.H. Kim, H.J. Lee, B. Hwang and H.M. Joo, Ocean Sci. J. 50 (2015) p.97.

[87] E.J. Davies, D. Buscombe, G.W. Graham and W.A.M. Nimmo-Smith, J. Atmos. Ocean Tech. 32 (2015) p.1241.

[88] W. Bishara, U. Sikora, O. Mudanyali, T.W. Su, O. Yaglidere, S. Luckhart and A. Ozcan, Lab Chip 11 (2011) p.1276.

[89] Y. Zhang, Y. Wu, Y. Zhang and A. Ozcan, Sci. Rep. 6 (2016) p.27811.

[90] A. Greenbaum, A. Feizi, N. Akbari and A. Ozcan, Opt. Express 21 (2013) p.12469.

[91] B. Khademhosseinieh, G. Biener, I. Sencan and A. Ozcan, Appl. Phys. Lett. 97 (2010) p.211112.

[92] S.O. Isikman, I. Sencan, O. Mudanyali, W. Bishara, C. Oztoprak and A. Ozcan, Lab Chip 10 (2010) p.1109.

[93] E. McLeod and A. Ozcan, Rep. Prog. Phys. 79 (2016) p.076001.

[94] S.L. Basedow, K.S. Tande, M.F. Norrbin and S.A. Kristiansen, Prog. Oceanogr. 108 (2013) p.72.

[95] R.J. Olson and H.M. Sosik, Limnol. Oceanogr-Meth 5 (2007) p.195.

[96] J.L. Wu, J.P. Li and R.K.Y. Chan, Opt. Express 21 (2013) p.14474.

[97] J.S. Erickson, N. Hashemi, J.M. Sullivan, A.D. Weidemann and F.S. Ligler, Anal. Chem. 84 (2012) p.839.

[98] J.M. Conley, J.G. Bradley, C.E. Giffen, A.L. Albey and A.D. Tomassian, Microbeam Anal. (1983) p. 177.

[99] J.A. Gaskin, G. Jerman, D. Gregory and A.R. Sampson, *Miniature variable pressure scanning electron microscope for in-situ imaging & chemical analysis, in IEEE Aerospace Conference Proceedings*, IEEE, New York, 2012, ISBN: 978-1-4577-0557-1.

[100] E.H. Adelson and J.Y.A. Wang, IEEE T. Pattern Anal. 14 (1992) p.99.

[101] M. Levoy, R. Ng, A. Adams, M. Footer and M. Horowitz, ACM Trans. Graphics 25 (2006) p.924.

[102] N. Streibl, Opt. Acta. 31 (1984) p.1233.

[103] N. Streibl, J. Opt. Soc. Am. A. 2 (1985) p.121.

[104] Y.Y. Schechner, N. Kiryati and R. Basri, Int. J. Comput. Vision 39 (2000) p.25.

[105] R. Ng and P. Hanrahan, Int. Opt. Des. Conf. 2006, Pts 1 and 2 6342 (2006) p.63421e.

[106] G.A. Zheng, R. Horstmeyer and C.H. Yang, Nat. Photonics 7 (2013) p.739.

[107] J.B. Chung, J. Kim, X.Z. Ou, R. Horstmeyer and C.H. Yang, Biomed. Opt. Express 7 (2016) p.352.

[108] S. Cazaux, A. Sadoun, M. Biarnes-Pelicot, M. Martinez, S. Obeid, P. Bongrand, L. Limozin and P.H. Puech, Ultramicroscopy 160 (2016) p.168.

[109] K. Haase and A.E. Pelling, J. R. Soc. Interface 12 (2015).

[110] J.M. Garcia-Ruiz, E. Nakouzi, E. Kotopoulou, L. Tamborrino and O. Steinbock, Sci. Adv. 3 (2017) p.e1602285.

[111] Y. Blanco, I. Gallardo-Carreno, M. Ruiz-Bermejo, F. Puente-Sanchez, E. Cavalcante-Silva, A. Quesada, O. Prieto-Ballesteros and V. Parro, Astrobiology 17 (2017) p.984.

[112] J.L. Nadeau, Y.B. Cho, J. Kuhn and K. Liewer, Frontiers Chem. 4 (2016) p.17.

[113] M.F. Toy, S. Richard, J. Kuhn, A. Franco-Obregon, M. Egli and C. Depeursinge, Biomed. Opt. Express 3 (2012) p.313.

[114] J.K. Wallace, S. Rider, E. Serabyn, J. Kuhn, K. Liewer, J. Deming, G. Showalter, C. Lindensmith and J. Nadeau, Opt. Express 23 (2015) p.17367.

[115] O. Mudanyali, C. Oztoprak, D. Tseng, A. Erlinger and A. Ozcan, Lab Chip 10 (2010) p.2419.